Journal of Hazardous Materials 185 (2011) 710–716

Contents lists available at ScienceDirect

Journal of Hazardous Materials

journal homepage: www.elsevier.com/locate/jhazmat

H_2O_2-sensitized TiO_2/SiO_2 composites with high photocatalytic activity under visible irradiation

Jian Zou[a,b,*], Jiacheng Gao[b]

[a] School of Chemistry and Chemical Engineering, Southwest University, Chongqing 400715, PR China
[b] College of Materials Science and Engineering, Chongqing University, Chongqing 400044, PR China

ARTICLE INFO

Article history:
Received 10 June 2010
Received in revised form 6 August 2010
Accepted 21 September 2010
Available online 1 October 2010

Keywords:
TiO_2/SiO_2
Visible light
Sensitizing
H_2O_2

ABSTRACT

TiO_2/SiO_2 composite photocatalysts were prepared by depositing of TiO_2 onto nano-SiO_2 particles. X-ray diffraction (XRD), transmission electron micrograph (TEM), Raman spectrometer, UV–Vis diffuse reflectance spectroscopy, Fourier transform infrared spectroscopy (FT-IR) were employed to characterize the properties of the synthesized TiO_2/SiO_2 composites. These results indicated that the products without calcination were amorphous, and calcination could enhance the crystallinity of TiO_2. Increases in the amount of TiO_2 would decrease the dispersion in the composites. H_2O_2-sensitized TiO_2/SiO_2 composite photocatalysts could absorb visible light at wavelength below 550 nm. The photocatalytic activity of as-prepared catalysts was characterized by methyl-orange degradation. The results showed the uncalcined composite photocatalysts with amorphous TiO_2 exhibited higher photocatalytic activity under visible light, and the activity of catalysts with TiO_2 content over 30% decreased with increasing of TiO_2 content. Increases in the calcination temperature and TiO_2 content promote the formation of bulk TiO_2 and result in a decrease in activity.

Crown Copyright © 2010 Published by Elsevier B.V. All rights reserved.

1. Introduction

Nanosized TiO_2 is one of the most promising photocatalysts. To achieve high activities in solution-phase catalysis the dispersion of the catalyst is very important. However, small particles tend to aggregate, resulting in lower or even completely lost photocatalytic activity. Although TiO_2 nanoparticles can be dispersed well in TiO_2 hydrosol, impurities or low pH values from TiO_2 precursors and peptizing agents can retard the oxidation of the substrate [1,2]. Supporting TiO_2 on high dispersing supporters is also another option to prevent agglomeration [3]. The SiO_2 particle is generally used as a supporter material [4–7]. Many supporting techniques in catalyst preparation have also been developed, and these as-made catalysts have different structures, configurations, and properties. The activity of catalysts shows significant differences. Enhancements in activity have been reported in several studies [4,7], but lower activities have also been reported by others [6].

Nanosized TiO_2 particles can be supported on monodisperse SiO_2 to prepare highly dispersed TiO_2/SiO_2 composites. However, the large SiO_2 core causes sedimentation of the catalysts, which leads to low photocatalytic activity [6]. High surface area and large pore volume are the most distinct strongpoints in enhancing the photocatalytic activity of TiO_2/SiO_2 composite catalysts. An amorphous TiO_2 phase is generally obtained for TiO_2/SiO_2 without calcinations. It was reported that amorphous TiO_2 was nearly inactive due to the facilitated recombination of the photoformed electron and hole [8]. Anatase is generally recognized to be the most active [9]. Highly crystalline anatase has high photocatalytic activity because of its reduced number of lattice defect sites. This limits the sites where electron–hole pairs could recombine [8,10]. It was well known that calcinations could enhance the crystallinity. Therefore, high-temperature calcination should be performed to obtain anatase phases with high crystallinity. However, the calcination could lower the surface area of catalysts and result in the agglomeration and growth of TiO_2, which is disadvantageous to enhancing activity of SiO_2/TiO_2 composite catalysts. Furthermore, the lack of absorption in the visible region of TiO_2/SiO_2 composites means that this catalyst cannot drive direct photocatalysis under visible light irradiation, thus lowering its photocatalytic activity under solar light irradiation.

The recombination of photogenerated electron–hole pairs must be restrained to enhance the activity of photocatalysts. As the particle size of TiO_2 nanoparticles decrease, the dominant recombination process of the charge carriers present surface recombination [11]. Thus, for small TiO_2 nanoparticles, the surface recombination would determine its photocatalytic activity. Many studies have

* Corresponding author at: School of Chemistry and Chemical Engineering, Southwest University, No. 2 Tiansheng Road, BeiBei District, Chongqing 400715, PR China. Tel.: +86 023 68252361; fax: +86 023 68252360.
E-mail address: ezouj@swu.edu.cn (J. Zou).

0304-3894/$ – see front matter. Crown Copyright © 2010 Published by Elsevier B.V. All rights reserved.
doi:10.1016/j.jhazmat.2010.09.077

confirmed that H_2O_2 can capture electrons to reduce the recombination process of the charge carriers [12–14]. More importantly, H_2O_2 molecules can adsorb onto the TiO_2 surface to form surface peroxide complexes, resulting in visible photoresponses [15–17]. In this study, SiO_2/TiO_2 composite catalysts are prepared by decorating monodisperse SiO_2 with TiO_2 without calcination. Hydrogen peroxide was used to modify the catalyst as the sensitizer. Highly visible activity is expected for H_2O_2-sensitized TiO_2/SiO_2 composites due to the synergetic effect of highly dispersed TiO_2 and sensitizing of H_2O_2.

2. Experimental

2.1. Materials

Titanium tetrachloride and tetraethyl orthosilicate (TEOS) were obtained in their reagent grade from Sinopharm Chemical Reagent Co. Ltd. (China). Ammonium hydroxide solution (25 wt%) and absolute ethanol were provided from Chengdu Kelong Chemical Reagent Co. (China). All of these materials were used as received.

2.2. Sample preparation

2.2.1. Preparation of SiO_2 sol

Silica particles were synthesized via the Stöber method [18]. The volume ratio of an ethanol/water/ammonium hydroxide/TEOS mixture was fixed at 60:10:1:6. The mixtures were stirred vigorously at 40 °C for 12 h, and then the prepared sol was diluted with 3 times volume of deionized water. The ethanol was distilled out from the boiling sol, after which the sol was condensed into the stock solution with 6 wt% SiO_2.

2.2.2. Preparation of TiO_2/SiO_2 composites

The TiO_2/SiO_2 particles were prepared by the deposition of TiO_2 from a $TiCl_4$ solution in the as-made SiO_2 sol. About 20 mL SiO_2 sol was diluted to 200 mL, followed by the addition of hydrochloric acid to adjust the pH of the solution to close to 1. A 0.5 M $TiCl_4$ solution was added to the SiO_2 sol and stirred vigorously for 30 min.A 10 wt% ammonium hydroxide solution was added dropwise into the SiO_2 sol to form a white precipitate with an ultimate aqueous mixture of pH 7–8. The product was obtained by filtration–washing cycles, dried at 100 °C, and calcined at different temperatures for 1 h. The resulted samples were denoted as *x*%TiO_2-*T*, and the samples without calcinations was denoted *x*%TiO_2, where *T* refers to the calcination temperature and *x* refers to the weight ratio of TiO_2/SiO_2. For comparison, the pure TiO_2 was acquired by precipitating the $TiCl_4$ solution with ammonium hydroxide solution, and the 10%TiO_2-H sample was obtained by increasing the process of refluxing and hydrolyzing $TiCl_4$ solution in the as-made SiO_2 sol at 95 °C for 5 h before the ammonium hydroxide solution was added.

The H_2O_2-sensitizing suspensions were made by adding 1 g powders into 10 mL 30% H_2O_2 and sonicating for 10 min. The suspensions were centrifuged, and the resulted powders was dried at room temperature and analyzed by UV–Vis spectroscopy.

2.3. Photocatalytic experiments

The photocatalytic activities of the samples were measured by the degradation of methyl orange (MO) in an aqueous solution. MO, a well-known acid–base indicator, is one of the series of common azo dyes largely used in the industry. MO is used as the model compound because it is difficult to remove and its concentration can be monitored by spectrophotometry [4,15]. A 2 mL H_2O_2-sensitizing suspension (containing 0.2 g catalysts) was diluted by the addition of 178 mL deionized water and 20 mL aqueous solution of MO (200 mg L^{-1}). A 450 W high pressure mercury lamp (Shanghai YaMin) with a filter was used as a visible-light source ($\lambda > 420$ nm). The suspension was stirred in the dark for 30 min in order to reach the adsorption–desorption equilibrium for MO before illumination, and its concentration was original concentration (C_o) of MO. After a given irradiation time, 5 mL suspensions were withdrawn, and the catalysts were separated from the suspensions by centrifugation at 5000 rpm without illumination. The concentration (C) of the residual MO in the solution was monitored by measuring the maximum absorbance of the upper clear solution using the UV–Vis spectrophotometer (Shimadzu UV-2550). All experiments were carried out at natural pH (about 5.1–5.8) without further adjustment. During the photocatalytic reaction, the temperature of the suspensions was maintained at ambient temperature (26–28 °C) by a circulating water bath.

2.4. Characterization

The phases of the products were characterized through X-ray diffraction method using CuK_α radiation ($\lambda = 0.15418$ nm) in a XD-3 diffractometer (Beijing Pgeneral). Transmission electron microscopy (TEM, Hitachi H7500) was performed at an accelerating voltage of 80 kV for electrons. Fourier transform infrared (FT-IR, Bruker TENSOR 27 FT-IR) spectra of TiO_2 powders were obtained using a spectrometer with KBr pellets technique. The Raman spectra were recorded on a Bruker RFS100 spectrometer with a resolution of 4 cm^{-1}, using 1054 nm light as an excitation source. The precision of the wavenumber was 1 cm^{-1}. The UV–Vis spectra were recorded on a spectrophotometer with an integrating sphere (Shmadzu UV-2550); $BaSO_4$ was used as a reference sample. The BET surface areas of samples were determined by N_2 adsorption–desorption method at 77 K using the 3H-2000I system (Beijing HuiHaiHong Nano-ST).

3. Results and discussions

3.1. Structure and morphology

3.1.1. XRD of used samples

Fig. 1 shows the XRD patterns of the SiO_2/TiO_2 powders fabricated by precipitation progress and by hydrolysis method. The X-ray powder diffraction patterns of the uncalcined precipitated powders show no crystalline TiO_2 phase peaks but have a very broad band from 15° to 30°, which is associated with amorphous SiO_2 [19]. Similar XRD patterns for samples containing different TiO_2 contents reveal that direct precipitation results in amorphous TiO_2 (the patterns were not exhibited here). A weak peak at

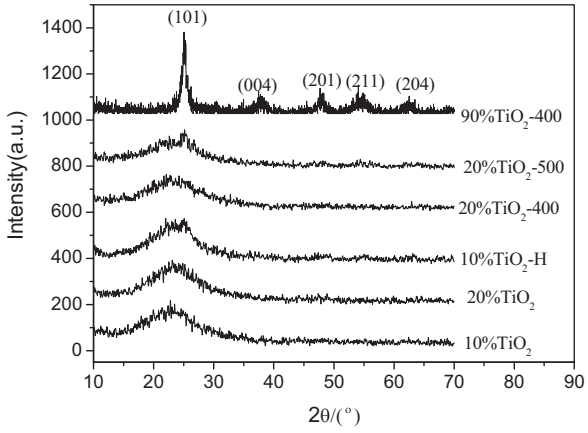

Fig. 1. XRD pattern of used samples.

$2\theta = 25.2^\circ$ appearing in 20%TiO_2-500 signifies that the amorphous TiO_2 was transformed into anatase after calcination at 500 °C. For 20%TiO_2-400, no anatase TiO_2 peak appeared. It is possible that the TiO_2 particles existed as particles smaller than 3 nm or that the characteristic peaks of TiO_2 were muffled by the diffraction peak of the SiO_2 amorphous phase due to the low TiO_2 amount [20]. Increased TiO_2 contents result in more crystalline anatase at lower temperatures, as confirmed by other peaks attributed to anatase TiO_2 besides the stronger peak at $2\theta = 25.2^\circ$ found in 90%TiO_2-400.

An additional peak at $2\theta = 25.2^\circ$, corresponding to the (1 0 1) of anatase TiO_2, was also observed for the hydrolyzed powders containing 10% TiO_2 (10%TiO_2-H). This showed that the hydrolysis method facilitated the formation of crystalline anatase TiO_2. It was reported [21] that the controlled crystalline phase TiO_2 could be prepared by the direct hydrolysis of $TiCl_4$ aqueous solutions at different temperatures, and higher temperatures are favorable for the formation of anatase. In this paper, the resulting products were anatase TiO_2 because the precursor of $TiCl_4$ aqueous solution was hydrolyzed at boiling and reflux conditions. Anatase is usually deemed to be the most photocatalytically active TiO_2 [9]. The activity of amorphous TiO_2 was nearly negligible due to the facilitated recombination of the photoformed electrons and holes at the traps on the surface and in the bulk of the particles [8]. To enhance the activity of the catalysts, TiO_2/SiO_2 composite powders prepared by typical methods must be calcined to form anatase TiO_2, because these samples were usually amorphous TiO_2. Thereby, the hydrolyzed TiO_2/SiO_2 powders may be also expected to have a high photocatalytic activity, due to the formation of anatase TiO_2.

3.1.2. Raman results

The phase structural complexity of the resulting photocatalyst could also be distinguished by Raman spectroscopy. Fig. 2 shows the Raman spectra of the samples prepared by hydrolysis method and by precipitation progress. The observed peaks at 144, 400, 515, and 639 cm^{-1} for 20%TiO_2-500 were attributed to the characteristics of the anatase phase [22]. This indicated that the anatase is the predominant phase structure. Some anatase was present in both 20%TiO_2-400 and 10%TiO_2-H, as confirmed by the lowest frequency Raman band observed in their spectra. The intensity of peaks for 20%TiO_2-500 is dramatically stronger than for others, indicating better crystallization. In addition, no such bands were detected in 20%TiO_2 and 10%TiO_2, which shows that amorphous TiO_2 is formed, as confirmed by XRD analysis. The nanoparticle size may be determined from measurements of the maximum lowest-frequency mode of the samples. The small size effect of the particle could cause a blue shift in the location of the Raman peaks [22]. Comparing the lowest frequency peaks of the crystalline samples, a blue shift is observed for 20%TiO_2-400, as shown in the inset in Fig. 2. This suggests that the particle sizes of TiO_2 for 20%TiO_2-400 were small.

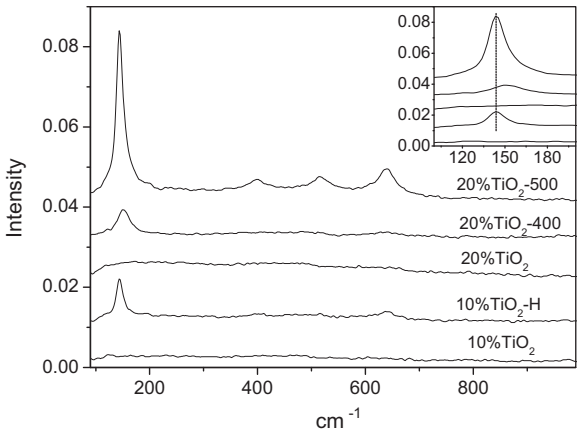

Fig. 2. Raman spectra of used samples (inset: the lowest-frequency spectra of the Egψ mode).

3.1.3. Morphologies of TiO_2 on the SiO_2 surface

TEM micrographs of the as-prepared samples are presented in Fig. 3. As seen from Fig. 3a, the pure SiO_2 possesses a regular spherical morphology and smooth surface, and the sizes of SiO_2 monodisperse particles are about 15–40 nm (Fig. 3a). For the precipitated SiO_2/TiO_2 composites, an irregular and rough surface is observed (Fig. 3b–d). This trend is even more evident as the TiO_2 loading increases, which indicates that TiO_2 particles were loaded onto the surface of SiO_2. Comparing Fig. 3b–d, it was found that more TiO_2 did not necessarily directly cover the surface of SiO_2 with increasing amounts of TiO_2 loading. Furthermore, the large numbers of SiO_2/TiO_2 composite particles at TiO_2 loadings less than 30% (including 30%) are monodisperse. However, the dispersion decreases with increasing TiO_2 loading, and monodisperse particles are no longer observed for 90%TiO_2 (Fig. 3d). This indicates the lower TiO_2 loading is more advantageous to the dispersion of SiO_2/TiO_2 composites prepared by direct precipitation progress. Calcined at 500 °C, 20%TiO_2 presents a smoother surface, and no dispersed small TiO_2 is observed (Fig. 3e). The possible reason was that thermal treatment might have resulted in the growth of dispersed TiO_2 and coating on the surface of SiO_2. In addition, hydrolyzed SiO_2/TiO_2 composites (Fig. 3f) exhibit differences in morphologies. There is an increase in isolated TiO_2 particles anchored on the surface of SiO_2 and the surface of SiO_2 is smoother.

3.1.4. Infrared spectroscopy

The IR spectra of silica loading TiO_2 are shown in Fig. 4. The bands at 1102, 800 and 469 cm^{-1} are due to asymmetric stretching, symmetric stretching, and the bending modes of Si–O–Si, respectively [23]. Bands around 950 cm^{-1} are presented in the spectra of all samples except for 90%TiO_2. As a consequence of the interaction between silica surface hydroxyls and titanium ions, a Si–O–Ti linkage of a band in this region (940–960 cm^{-1}) would be formed [23]. This band is often considered to be the fingerprint of the titania deposition on the silica.

Bands at 615 cm^{-1} were detected in all samples. This band could be attributed to the TiO_2 bulk phase [23]. The evolution of this band obviously was depicted during thermal treatment of the samples to higher temperatures (Fig. 4, curves b–d). The results of Raman indicated that the thermal treatment resulted in the transformation of amorphous TiO_2 to anatase TiO_2 and the growth of TiO_2 nanoparticles. Zeleňák et al. [23] also attributed the evolution to the decrease in dispersion and growth of the TiO_2 particles. The formation of bulk TiO_2 comes at the expense of vanishing Ti–O–Si linkages, as shown in the increase in intensity of the 615 cm^{-1} band and the decrease in the 950 cm^{-1} band for 20%TiO_2-500 (Fig. 4, curve d). Furthermore, both bands at 615 and 950 cm^{-1} are also observed for 10%TiO_2-H (Fig. 4, curve e). Considering these, a possible structure for 10%TiO_2-H composite is a heterojunction consisting of the isolated TiO_2 anchored onto the silica by Ti–O–Si linkages. The spectrum of 30%TiO_2 presents a more intense band at 615 cm^{-1} compared to that of 20%TiO_2, indicating that the increase in TiO_2 results in the formation of bulk TiO_2 agglomeration. This is supported by the spectrum of 90%TiO_2. The 615 cm^{-1} band evolves into a wide band between 700 and 400 cm^{-1} while the 950 cm^{-1} band becomes negligible. The TEM map confirms the existence of TiO_2 agglomeration in 90%TiO_2.

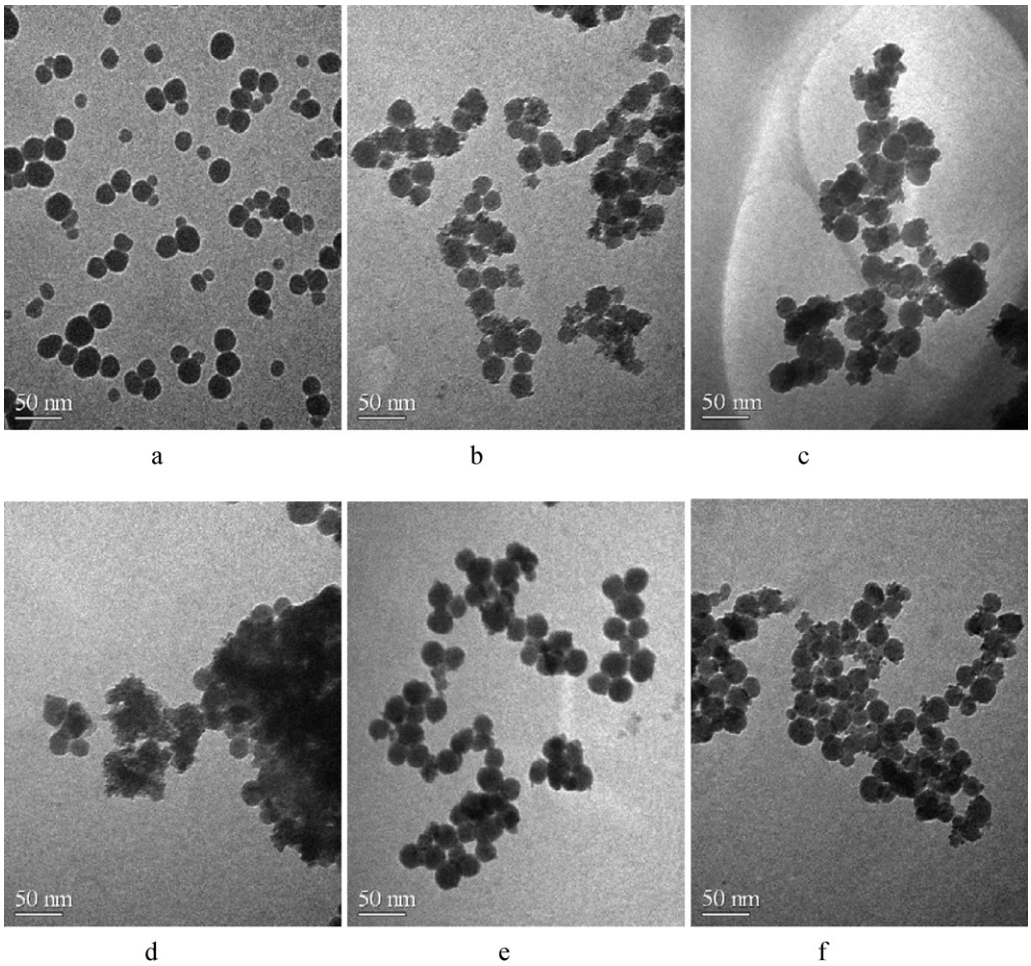

Fig. 3. TEM photographs of the samples (a) SiO_2; (b) 20%TiO_2; (c) 30%TiO_2; (d) 90%TiO_2; (e) 20%TiO_2-500; (f) 10%TiO_2-H.

3.2. UV–Vis spectra

Fig. 5 shows the UV–Vis absorption of used samples before and after treatment with H_2O_2. As shown in Fig. 5a, pure SiO_2 hardly absorbs UV light. However, a strong absorption is observed for the TiO_2/SiO_2 composites, which corresponds to the absorption of TiO_2. And as the TiO_2 loading increases, a progressive increase of the UV absorption is observed. It is well known that neither SiO_2 nor TiO_2 can absorb visible light due to their wide energy gaps. It also can be confirmed from Fig. 5a that no sample displayed an observable absorption in the visible region (wavelength $\lambda > 420$ nm). This shows that TiO_2/SiO_2 composites without any treatments cannot drive the direct photocatalysis under visible light irradiation.

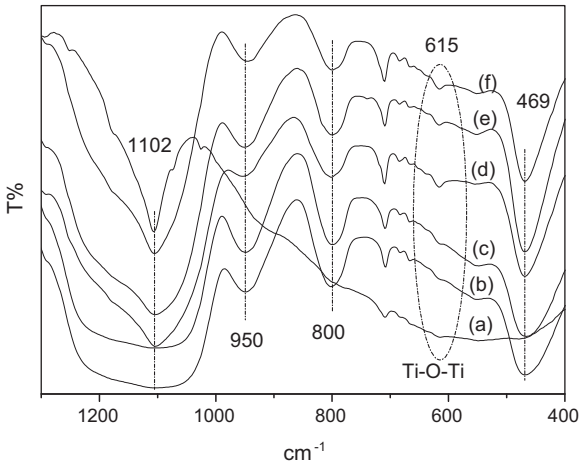

Fig. 4. IR spectra of used samples. (a) 90%TiO_2; (b) 20%TiO_2; (c) 20%TiO_2-400; (d) 20%TiO_2-500; (e) 10%TiO_2-H; (f) 30%TiO_2.

TiO_2 treated with H_2O_2 can absorb visible light to some extent due to the formation of peroxo complexes between Ti and H_2O_2 [15]. The UV–Vis absorption of the samples treated with H_2O_2 is shown in Fig. 5b. Compared to the absorption spectra in Fig. 5a, the ones in Fig. 5b present a significant difference. A new absorption in the visible range of 400–550 nm is observed for all TiO_2/SiO_2 composites after treatment with H_2O_2 in addition to the UV absorption edge. This indicates that peroxo complexes are formed on the TiO_2/SiO_2 composites. It can also be seen that the increased TiO_2 can improve the visible absorption but it is not proportional to the increase in the amount of TiO_2 loading. TiO_2/SiO_2 composites with TiO_2 loads varying from 20% to 70% present the similar visible absorption. It should be noted that lower visible absorption is observed for TiO_2/SiO_2 composites (10%TiO_2-H) prepared by hydrolysis method, although its TiO_2 loading content was as much as that of the 10% TiO_2 sample prepared by precipitation progress. The visible absorption of TiO_2/SiO_2 composites results from the formation of Ti–peroxo complexes because no visible absorption is detected for H_2O_2-treated SiO_2.

Efficient irradiation is indispensable for the photocatalysis of catalysts. The transmittance of catalyst suspensions can influence the irradiation on inner catalysts in the suspension. An increase in

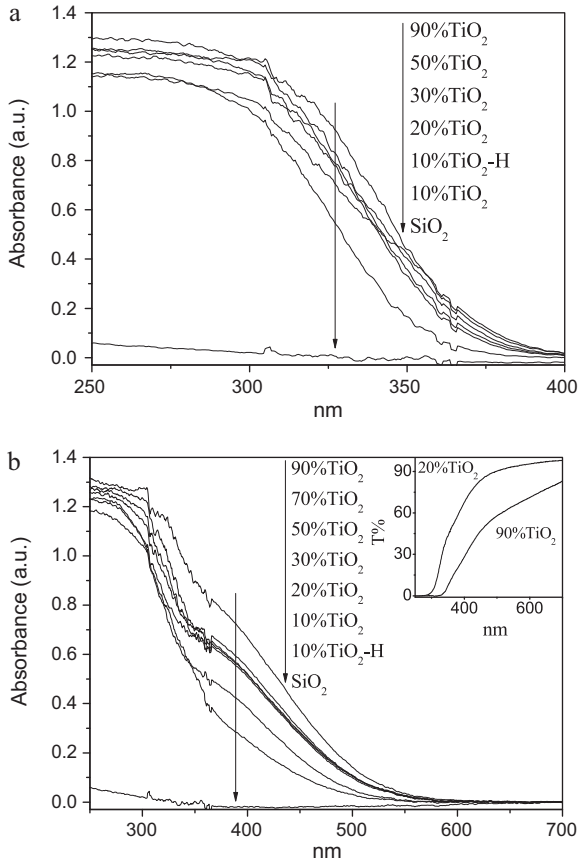

Fig. 5. Diffusion reflection absorption of used samples untreated (a) and treated (b) with H_2O_2 (figure b inset: the transmittance of 20%TiO_2 and 90%TiO_2).

TiO_2 loading results in a decrease in transmittance, as observed in the TiO_2/SiO_2 composite suspensions. The transmittances for 20%TiO_2 and 90%TiO_2 are shown in Fig. 5b. It is obvious that the transmittance for 20%TiO_2 suspension is much higher than that of the 90%TiO_2 suspension. The transmittance at 420 nm was about 75% for 20%TiO_2 but only 36% for 90%TiO_2. This maybe is attributed to the higher absorption at 420 nm for 90%TiO_2. However, at 550 nm, where these two catalysts have the same absorbance, a transmittance of up to 94% was detected for the 20%TiO_2 suspension, while that of the 90%TiO_2 suspension is only 75%. This may be due to the formation of large sized aggregates in 90%TiO_2 (Fig. 3d). The large aggregates would decrease the transmittance of the suspension [24]. This indicates that the inner catalysts in 20%TiO_2 suspension may be excited more efficiently than those in the 90%TiO_2 suspension.

3.3. Photocatalytic experiments

Photocatalytic activity tests were investigated by the degradation of methyl orange (MO) in aqueous solution under visible light irradiation. Fig. 6 presents the photocatalytic results of the as-prepared TiO_2/SiO_2 composites treated with H_2O_2 under visible light irradiation. H_2O_2 alone cannot drive the direct photocatalysis under visible light irradiation, as shown in Fig. 6a. Pure TiO_2 displays much lower photocatalytic activity when compared to TiO_2/SiO_2 composites. Previous studies have that the high visible activity is observed only for sulfated TiO_2 [15]. However, the remarkable enhancement of activity is presented for TiO_2/SiO_2 composite photocatalysts, and the highest activities are observed for 20%TiO_2 and 30%TiO_2.As the TiO_2 loading increased to over 30%, a progressive decrease in activity is presented.

Fig. 6b shows the activity of crystalline TiO_2/SiO_2 composites. P25 without H_2O_2, which was used as a reference, shows only 6% discoloration after 150 min, which hints that the effect of dye sensitization [25] from MO was extremely limited. Anatase is usually deemed to be the most photocatalytically active TiO_2, and high crystallinity results in higher activity [4]. Crystalline 20%TiO_2 photocatalysts display a progressive decrease in activity as the temperatures of thermal treatment increased compared to amorphous 20%TiO_2. This is explained by improved crystallization as shown in XRD and Raman spectra. No degradation of MO even is observed for anatase 10%TiO_2-H, but about 95% discoloration is detected for amorphous 10%TiO_2, as seen in Fig. 6a. For P25 with H_2O_2, a lower discoloration rate is observed (about 37%), although high crystallinity and synergistic effects were also observed [5]. Previous research indicates that P25 in acidic solutions has high activity [15]. Lower pH could promote the degradation of the MO [26]. However, in this study, all experiments were carried out at pH 5–6, at which the kinetic constant values of MO are changed little [26]. The pH values are nearly unaltered during all reactions. Therefore, the pH values have nearly no influence on the photocatalytic activity.

Typically, the addition of silica can enhance the photocatalytic activity of TiO_2/SiO_2 catalysts [4,7]. However, these catalysts cannot drive direct photocatalysis under visible light irradiation due to the lack of adsorption of visible light of undoped TiO_2 or SiO_2. TiO_2/SiO_2 composite catalysts treated only with H_2O_2 have high activity under visible light irradiation, as shown in Fig. 6. Catalysts treated with H_2O_2 can absorb visible light due to the formation of peroxo complexes between H_2O_2 and Ti ions, as seen in Fig. 5. This

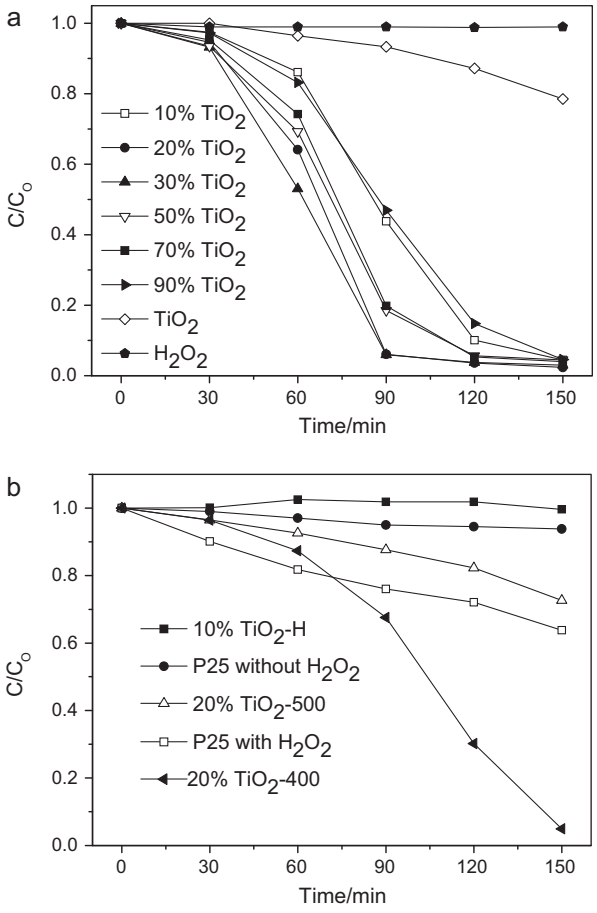

Fig. 6. Photocatalytic activities of amorphous TiO_2 (a) and crystalline TiO_2 treated with H_2O_2 under visible light ($\lambda > 420$ nm).

Table 1
The surface area of the used samples.

	Sample				
	SiO_2	10%TiO_2	30%TiO_2	90%TiO_2	TiO_2
Surface area (m^2/g)	46.8	53.8	42.7	26.7	20.3

indicates that catalysts can directly drive the visible photocatalysis. It was reported that the photocatalyzed epoxidation of olefin [16] and the degradations of salicylic acid [17] and MO [15] were fulfilled by TiO_2 treated with H_2O_2 under visible irradiation. Peroxo complexes are responsible for the visible activity of TiO_2/SiO_2 composites treated with H_2O_2, and the increase of TiO_2 content may form more peroxide complexes that result in stronger visible absorption as shown in Fig. 5b, which means catalysts have more high activity. However, as shown in Fig. 6a, it is observed that the trend in catalytic activity is not entirely linear with the increase in TiO_2 content. At TiO_2 contents above 20%, the activity decreases as TiO_2 loading increases. From the TEM map, 20%TiO_2 shows a highly dispersed phase, but 90%TiO_2 forms aggregates. It is well known that highly dispersed phases facilitate high activity. Mesoporous SBA-15 with higher Ti/Si ratios has lower activity because TiO_2 aggregates and forms large clusters with increasing Ti content [27]. Titanium–silicon binary oxide catalysts have high photocatalytic activity due to highly dispersed tetrahedral titanium oxide species [28]. Moreover, the inset of Fig. 5b shows that inner catalysts could be excited by visible light, as confirmed by the higher transmittance observed for catalyst with lower TiO_2 content. Thus, the effective utilization rate is lower for catalyst with higher TiO_2 loading, resulting in the low activity. Compared to P25, Zhao et al. found that as-prepared TiO_2 had higher photocatalytic activities, because the latter had higher transmittance, which resulted in less radiation loss [29].

The addition of silica to TiO_2 photocatalysts can facilitate the enhancement of their specific surface area, which would provide more surface sites for the adsorption of reactants molecules and result in the enhancement of photocatalytic activity [30]. Table 1 shows the specific surface area of used samples. A progressive increase in surface area is achieved as the TiO_2 loading decreased. The adsorption of MO on photocatalysts is shown in Fig. 7. The progressive decrease of the absorption rate of MO is observed as the TiO_2 loading increased, which is in agreement with the surface areas in Table 1. A decrease in absorption rate is observed in 10%TiO_2-H, even though it has the same TiO_2 content as 10%TiO_2. These could be attributed to the existence of some TiO_2 aggregations on the silica for catalysts with higher TiO_2 content and 10%TiO_2-H, as shown in the TEM and IR results. Moreover, the trend in catalytic activity is similar to the absorption capability of catalysts as the TiO_2 loading rose to above 20%, as seen in Figs. 6b and 7. The highest adsorption rate is observed for 10%TiO_2, but lower activity is depicted when compared to TiO_2/SiO_2 composites. This may be due to that an excessively small amount of TiO_2 is not conducive to the formation of peroxide complexes, resulting in lower visible absorption as depicted in Fig. 5b.

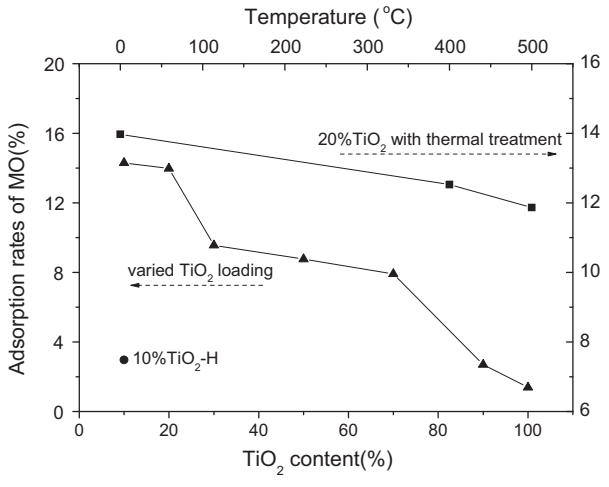

Fig. 7. The adsorption rate of MO on used samples.

Figs. 6 and 7 indicate a dramatic decrease in activity for 20%TiO_2 with calcination although the adsorption rate of 20%TiO_2 with thermal treatment decreased slightly, especially for 20%TiO_2-500. This implies that amorphous TiO_2 has higher photocatalytic activity. The thermal treatment results in the transformation of amorphous TiO_2 to anatase TiO_2, and the increase in calcined temperature results in better crystallization, as confirmed by XRD and Raman spectroscopy.

Anatase is more photocatalytically active than the rutile and amorphous TiO_2 [9]. Amorphous TiO_2 is nearly inactive due to the facilitated recombination of photoformed electrons and holes [8]. Some reports also attribute high activity to high anatase content for TiO_2/SiO_2 composites [31]. Besides, the specific surface area, crystal composition, and material microstructures also significantly affect the catalytic performance of TiO_2. Wang et al. [32] found that the crystallinity of the photocatalysts was less influential than the nitrogen content in determining the photocatalytic activity of N-doped TiO_2. Li et al. [33] prepared the amorphous hcp TiO_2 nanocolumn arrays, which have better photocatalytic properties than anatase nanocolumn arrays. Our previous study also showed that amorphous TiO_2 sol had higher photocatalytic activity than anatase sol [34]. In this study, it was proven that thermal treatments can result in the formation of bulk TiO_2 and growth of TiO_2 molecules as confirmed by IR and Raman results, which decrease the dispersion of TiO_2. This high dispersion contributes to higher activity because the high dispersion of TiO_2 facilitates the interaction between TiO_2 and other species, including H_2O_2, SiO_2 and reactant molecules. This is particularly evident for anatase 10%TiO_2-H. No activity was observed due to the existence of bigger TiO_2 particles although TiO_2 was anatase phase. The results above suggest that the enhancement of photocatalytic activity is dictated more by the dispersion of TiO_2 than its crystal structure.

4. Conclusions

Highly dispersed TiO_2/SiO_2 composite catalysts were prepared by decorating monodisperse SiO_2 nanoparticles with a small quantity of TiO_2. Enhanced visible activity was found in for TiO_2/SiO_2 composites sensitized with H_2O_2. Composite catalysts without calcination and with low TiO_2 content showed higher activity even though TiO_2 was amorphous. The High transmittance of catalyst suspensions could enhance effective utilization rate of a light source. This shows that less TiO_2 can achieve a higher degradation rates. Therefore, Composites catalysts without calcination and with low TiO_2content are inexpensive and conducive to the practical application of catalysts in the treatment of pollutants.

Acknowledgments

The work described in this paper was supported by a grant from the doctor foundations of Southwest University (SWU109017) and the fundamental research funds for the Central Universities (XDJK2009C097).

References

[1] S. Yamazaki, N. Nakamura, Photocatalytic reactivity of transparent titania sols prepared by peptization of titanium tetraisopropoxide, J. Photochem. Photobiol. A 193 (2008) 65–71.

[2] S.S. Watson, D. Beydoun, J.A. Scott, R. Amal, The effect of preparation method on the photoactivity of crystalline titanium dioxide particles, Chem. Eng. J. 95 (2003) 213–220.

[3] M.R. Hoffmann, S.T. Martin, W. Choi, D.W. Bahnemann, Environmental applications of semiconductor photocatalysis, Chem. Rev. 95 (1995) 69–96.

[4] X. Jiang, T. Wang, Influence of preparation method on morphology and photocatalysis activity of nanostructured TiO_2, Environ. Sci. Technol. 41 (2007) 4441–4446.

[5] S.H. Lim, N. Phonthammachai, S.S. Pramana, T.J. White, Simple route to monodispersed silica–titania core-shell photocatalysts, Langmuir 24 (2008) 6226–6231.

[6] P. Wilhelm, D. Stephan, Photodegradation of rhodamine B in aqueous solution via SiO_2@TiO_2 nano-spheres, J. Photochem. Photobiol. A 185 (2007) 19–25.

[7] X. Song, L. Gao, Fabrication of hollow hybrid microspheres coated with silica/titania via sol–gel process and enhanced photocatalytic activities, J. Phys. Chem. C 111 (2007) 8180–8187.

[8] B. Ohtani, Y. Ogawa, Nishimoto, S, Photocatalytic activity of amorphous-anatase mixture of titanium(IV) oxide particles suspended in aqueous solutions, J. Phys. Chem. B 101 (1997) 3746–3752.

[9] T. Ohno, K. Sarukawa, M. Matsumura, Photocatalytic activities of pure rutile particles isolated from TiO_2 powder by dissolving the anatase component in HF solution, J. Phys. Chem. B 105 (2001) 2417–2420.

[10] K. Tanaka, M.F.V. Capule, T. Hisanaga, Effect of crystallinity of TiO_2 on its photocatalytic action, Chem. Phys. Lett. 187 (1991) 73–76.

[11] X. Chen, S.S. Mao, Titanium dioxide nanomaterials: synthesis, properties, modifications, and applications, Chem. Rev. 107 (2007) 2891–2959.

[12] J. Fernández, J. Kiwi, J. Baeza, J. Freer, C. Lizama, H.D. Mansilla, Orange II photocatalysis on immobilised TiO_2 effect of the pH and H_2O_2, Appl. Catal. B 48 (2004) 205–211.

[13] H.K. Singh, M. Saquib, M.M. Haque, M. Muneer, Heterogeneous photocatalyzed degradation of uracil and 5-bromouracil in aqueous suspensions of titanium dioxide, J. Hazard. Mater. 142 (2007) 425–430.

[14] M.A. Barakat, J.M. Tseng, C.P. Huang, Hydrogen peroxide-assisted photocatalytic oxidation of phenolic compounds, Appl. Catal. B 59 (2005) 99–104.

[15] J. Zou, J. Gao, Y. Wang, Synthesis of highly active H_2O_2-sensitized sulfated titania nanoparticles with a response to visible light, J. Photochem. Photobiol. A 202 (2009) 128–135.

[16] X. Li, C.C. Chen, J.C. Zhao, Mechanism of photodecomposition of H_2O_2 on TiO_2 surfaces under visible light irradiation, Langmuir 17 (2001) 4118–4122.

[17] T. Ohno, Y. Masaki, S. Hirayama, M. Matsumura, TiO_2-photocatalyzed epoxidation of 1-decene by H_2O_2 under visible light, J. Catal. 204 (2001) 163–168.

[18] H. Flachsbart, W. Stöber, Preparation of radioactively labeled monodisperse silica spheres of colloidal size, J. Colloid Interface Sci. 30 (1969) 568–573.

[19] G. Liu, Y. Liu, G. Yang, S. Li, Y. Zu, W. Zhang, M. Jia, Preparation of titania–silica mixed oxides by a sol–gel route in the presence of citric acid, J. Phys. Chem. C 113 (2009) 9345–9351.

[20] Z. Wang, F. Zhang, Y. Yang, B. Xue, J. Cui, N. Guan, Facile postsynthesis of visible-light-sensitive titanium dioxide/mesoporous SBA-15, Chem. Mater. 19 (2007) 3286–3293.

[21] H.D. Nam, B.H. Lee, S.J. Kim, C.H. Jung, J.H. Lee, S. Paek, Preparation of ultrafine crystalline TiO_2 powders from aqueous $TiCl_4$ solution by precipitation, Jpn. J. Appl. Phys. 37 (1998) 4603–4608.

[22] S. Kelly, F.H. Pollak, M. Tomkiewicz, Raman spectroscopy as a morphological probe for TiO_2 aerogels, J. Phys. Chem. B 101 (1997) 2730–2734.

[23] V. Zeleňák, V. Hornebecq, S. Mornet, O. Schäf, P. Llewellyn, Mesoporous silica modified with titania: structure and thermal stability, Chem. Mater. 18 (2006) 3184–3191.

[24] S. Yurdakal, V. Loddo, B.B. Ferrer, G. Palmisano, V. Augugliaro, J.G. Farreras, L. Palmisano, Optical properties of TiO_2 suspensions: influence of pH and powder concentration on mean particle size, Ind. Eng. Chem. Res. 46 (2007) 7620–7626.

[25] B. Ohtani, Preparing articles on photocatalysis beyond the illusions, misconceptions, and speculation, Chem. Lett. 37 (2008) 217–229.

[26] V. Augugliaro, C. Baiocchi, A.B. Prevot, E. García-López, V. Loddo, S. Malato, G. Marcí, L. Palmisano, M. Pazzi, E. Pramauro, Azo-dyes photocatalytic degradation in aqueous suspension of TiO_2 under solar irradiation, Chemosphere 49 (2002) 1223–1230.

[27] G. Li, X.S. Zhao, Characterization and photocatalytic properties of titanium-containing mesoporous SBA-15, Ind. Eng. Chem. Res. 45 (2006) 3569–3573.

[28] H. Yamashita, S. Kawasaki, Y. Ichihashi, M. Harada, M. Takeuchi, M. Anpo, G. Stewart, M.A. Fox, C. Louis, M. Che, Characterization of titanium-silicon binary oxide catalysts prepared by the sol–gel method and their photocatalytic reactivity for the liquid-phase oxidation of 1-octanol, J. Phys. Chem. B 102 (1998) 5870–5875.

[29] Y. Zhao, C. Li, X. Liu, F. Gu, Highly enhanced degradation of dye with well-dispersed TiO_2 nanoparticles under visible irradiation, J. Alloys Compd. 440 (2007) 281–286.

[30] Y. Li, S. Kim, Synthesis and characterization of nano titania particles embedded in mesoporous silica with both high photocatalytic activity and adsorption capability, J. Phys. Chem. B 109 (2005) 12309–12315.

[31] X. Yang, D. Yang, H. Zhu, J. Liu, W.N. Martins, R. Frost, L. Daniel, Mesoporous structure with size controllable anatase attached on silicate layers for efficient photocatalysis, J. Phys. Chem. C 113 (2009) 8243–8248.

[32] J. Wang, W. Zhu, Y. Zhang, S. Liu, An efficient two-step technique for nitrogen-doped titanium dioxide synthesizing: visible-light-induced photodecomposition of methylene blue, J. Phys. Chem. C 111 (2007) 1010–1014.

[33] Y. Li, T. Sasaki, Y. Shimizu, N. Koshizaki, Hexagonal-close-packed, hierarchical amorphous TiO_2 nanocolumn arrays: transferability, enhanced photocatalytic activity, and superamphiphilicity without UV irradiation, J. Am. Chem. Soc. 130 (2008) 14755–14762.

[34] J. Zou, J. Gao, F. Xie, An amorphous TiO_2 sol sensitized with H_2O_2 with the enhancement of photocatalytic activity, J. Alloys Compd. 497 (2010) 420–427.